Joint Nanoscale Communication and Sensing Enabled by Plasmonic Nano-antennas

Amit Sangwan
amit@northeastern.edu
Ultrabroadband Nanonetworking Laboratory
Institute for the Wireless Internet of Things
Northeastern University
Boston, Massachusetts, USA

Josep Miquel Jornet
jmjornet@northeastern.edu
Ultrabroadband Nanonetworking Laboratory
Institute for the Wireless Internet of Things
Northeastern University
Boston, Massachusetts, USA

ABSTRACT

With the advances in nanotechnology, novel nanosensing technologies can play a pivotal role in today's society. Plasmonic sensing has been proven to provide unprecedented detection reliability and resolution in a very compact form factor. Traditional plasmonic sensors leverage biofunctionalized metallic grating structures whose frequency response in transmission and/or reflection changes according to the presence of targeted biomarkers. However, these sensing setups require the use of bulky measurement equipment to couple light to and from sensors for excitation and detection. In parallel, for over a decade, the nanoscale electromagnetic communication community has been leveraging plasmonic structures to efficiently transmit information at the nanoscale. By combining the two realms, in this paper, the concept of joint nanoscale communication and sensing enabled by plasmonic sensing nano-antennas is proposed. First, the changes in the frequency response of a biofunctionalized plasmonic nano-antenna when exposed to different biomarkers are modeled. Then, a chirp-spread spectrum excitation and detection system is proposed as a way to enable simultaneous communication and sensing at the nanoscale. Numerical results are provided to demonstrate the performance of the proposed system.

CCS CONCEPTS

• **Computer systems organization** → **Sensors and actuators**.

KEYWORDS

Nano-sensing antenna, Nano-communication, Plasmonics, Intra-body communication

ACM Reference Format:
Amit Sangwan and Josep Miquel Jornet. 2021. Joint Nanoscale Communication and Sensing Enabled by Plasmonic Nano-antennas. In *The Eight Annual ACM International Conference on Nanoscale Computing and Communication (NANOCOM '21), September 7–9, 2021, Virtual Event, Italy*. ACM, New York, NY, USA, 6 pages. https://doi.org/10.1145/3477206.3477447

NANOCOM '21, September 7–9, 2021, Virtual Event, Italy

ACM ISBN 978-1-4503-8710-1/21/09…$15.00
https://doi.org/10.1145/3477206.3477447

1 INTRODUCTION

With the most ever-connected world, early detection and diagnosis of diseases play a pivotal role in the entire community's health. In this context, current sensing technologies must be advanced to a more compact and mass-producible design for widespread availability and use-case scenarios. In light of the COVID-19 pandemic, the need for more compact and easier to deploy sensing mechanisms has been more evident than ever [8]. Innovative sensing technologies can play a key role in preventing future pandemics.

Sensing of disease-specific biomarkers can be performed using several methodologies [12, 15]. These include the use of color-changing chemicals (i.e., titration), spectroscopy, antigens tests, and other recent genetic techniques (e.g., RNA/DNA sequencing). These advances have led to tools to examine and detect biological specimens with unprecedented accuracy. However, currently, such setups generally rely on bulky and expensive test equipment.

In parallel to these advances, nanotechnology has provided us with tools to design devices at the nanoscale and engineer structures with nanometer-level accuracy. Plasmonic biosensing [6, 14, 17] is one such field, which takes advantage of the surface plasmon resonance (SPR) for the detection of the biomarkers at the nanoscale. These sensors harness the molecular interactions happening at the nanoscale and offer exceptional precision. State-of-the-art plasmonic sensors mostly rely on grating structures to couple incident light to SPR waves. Although these designs rely on a simple process of reflection to perform sensing, the operation of these sensors often involves using bulky equipment to couple light to and from the sensor for measurements, confined to laboratory settings.

Alongside, nanoscale electromagnetic (EM) communication networks [1] offer a compact form factor to transmit and receive information (e.g., generated by nanosensors) by leveraging nano-antennas that rely on the very same SPR material properties. However, with the exception of only very few cases [16], the communication and sensing units of embedded nano-systems or nanomachines are considered separate elements.

In this paper, we introduce the concept of joint nanoscale communication and sensing enabled by plasmonic nano-antennas. More specifically, first, we propose a nano-patch antenna with a biofunctionalized surface that can also act as a sensing device. Figure 1 illustrates the design of the nano communicating and sensing antenna. The biofunctionalized layer on top of the antenna can be coated with a disease-specific biomarker detection layer that, when in the proximity of a biomarker, binds with it and changes its physical and electrochemical properties. On their turn, these trigger a change in the antenna frequency response. Second, we propose a

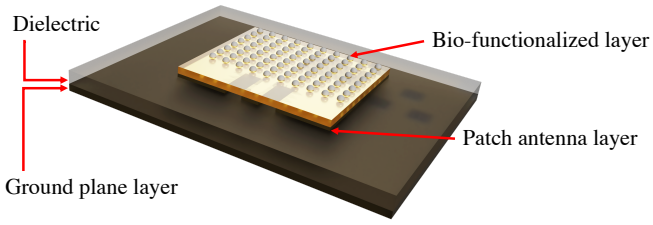

Figure 1: Concept of plasmonic nano-patch antenna as a bio-functionalized sensor.

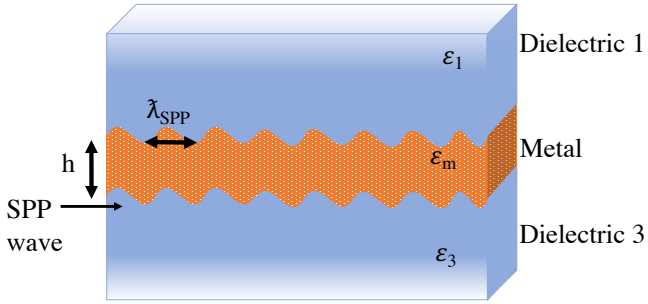

Figure 2: SPP waves at metal-dielectric-metal interfaces for thin metal.

chirp spread spectrum (CSS)-based scheme to practically enable simultaneous sensing and communication at the nanoscale. In particular, the EM signature of the sensing plasmonic nano-antenna is imprinted on the broadband CSS waveform, and can be detected at the receiver through different methods. In parallel, the transmitted chirps can be modulated according to the data to be transmitted in different ways (e.g., binary CSS or chirped-BPSK [11]).

The remainder of this paper is organized as follows. In Section 2, following the description of the material properties that govern the design of antennas at optical frequencies, we provide a reference design of an optical patch nano-antenna utilized in this paper. In Section 3, we explain the key principle of the nano-antenna working as a sensor and numerically illustrate it. In Section 4, we design the antenna excitation signal able to exploit its sensing properties and in Section 5 we propose strategies and architectures that can leverage the designed signals to perform the detection within a nano-machine design constraints. Finally, in Section 6, we present the results of numerical modelling demonstrating the detection performance and the distinction of binding versus non-binding states of the antenna at the detector based on the received signal. We conclude the paper in Section 7.

2 NANO ANTENNA DESIGN

2.1 Plasmonic properties of metals at optical frequencies

Optical nano-antennas function in a similar way to traditional EM antennas [9]. The only difference in design is due to the electrical properties of the materials at optical frequencies. Metals are perfect electric conductors at lower frequencies but exhibit complex-valued conductivity at optical frequencies. As a result, the plasmonic effects on the metallic antenna surfaces need to be considered while designing resonating structures. Surface plasmon polariton (SPP) waves are oscillations in the electron cloud present at the metal-dielectric interface. The Drude-Lorentz model describes this complex permittivity arising from such oscillations as a combination of the oscillator with a damping constant related to the complex-valued permittivity of the metal. This is given by [13]

$$\varepsilon_m = \left[\varepsilon_m(\infty) - \frac{\omega_p^2 \tau_d^2}{1+\omega^2\tau_d^2} + j\frac{\omega_p^2 \tau_d}{\omega\left(1+\omega^2\tau_d^2\right)}\right], \tag{1}$$

where ε_m is the permittivity of the metal, ω_p is the plasma frequency of the material, τ_d is the electron relaxation time, $\epsilon_m(\infty)$ is the high frequency dielectric constant and $\omega = 2\pi f$ is the angular frequency.

By solving for the propagation wave vector k_{spp}, we can determine the propagation of SPP waves while accounting for dispersion along the structure. In particular, for a planar structure, the complex-valued SPP wave vector, k_{spp}, can be obtained by solving [13]

$$k_{spp} = \left(\varepsilon_1\varepsilon_3 S_3^2 + \varepsilon_m^2 S_2 S_3\right)\tanh\left(S_2 h\right) + \varepsilon_m S_2\left(\varepsilon_3 S_1 + \varepsilon_1 S_3\right) \tag{2}$$

$$S_1 = \sqrt{\beta^2 - \varepsilon_1 k_0^2}, \tag{3}$$

$$S_2 = \sqrt{\beta^2 - \varepsilon_m k_0^2}, \tag{4}$$

$$S_3 = \sqrt{\beta^2 - \varepsilon_3 k_0^2}, \tag{5}$$

where $k_0 = \omega/c$ is the free space vector, β is the complex propagation constant parallel to the surface, ε_1 and ε_3 are the permittivity of the layers surrounding the metal sheet, and ε_m is the permittivity of the metal as described in (1). Using k_{spp}, we can calculate the plasmonic wavelength using the relation:

$$\lambda_{spp} = \frac{2\pi}{\Re\left\{k_{spp}\right\}}. \tag{6}$$

At optical frequencies, λ_{spp} governs the antenna design equations instead of the free space wavelength.

2.2 Optical nano-patch design

Patch antennas have found use in numerous applications demanding a compact form factor. The main advantage of using a patch antenna lies in its planar structure, making it easier to fabricate in large quantities and integrate with the rest of the system. A patch antenna consists of a resonating rectangular structure on a ground plane. The length of a perfect electric conductor patch L is chosen [2]such that $L > \lambda_0/3$ and $L < \lambda_0/2$, where λ_0 is the free-space wavelength. However, the exact values depend upon the dielectric material that confines the fields between the antenna and the ground plane. Patch antennas are usually designed as broadside radiators (i.e., maximum radiation in the direction normal to patch plane). However, depending upon the design and excitation mode choices, it can also be designed as an end-fire radiator (maximum radiation in the direction of the plane of the patch).

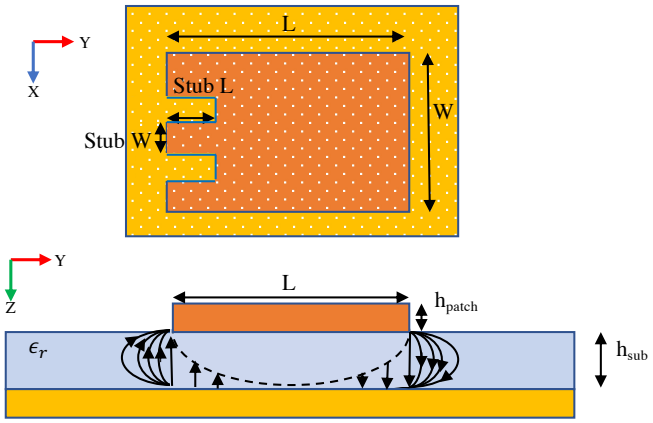

Figure 3: Geometry of a patch antenna.

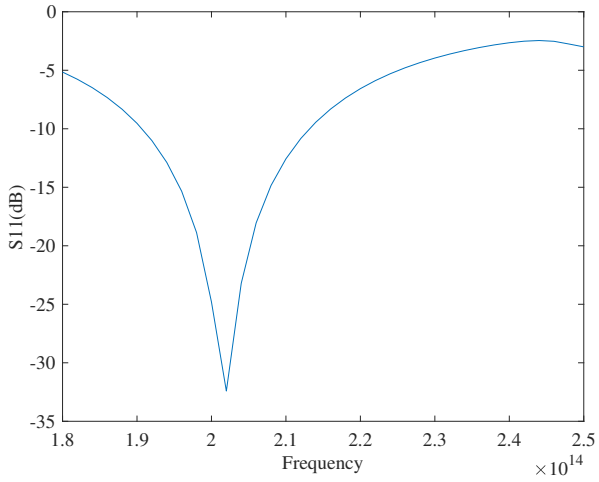

Figure 4: S11 parameter of the reference nano-patch antenna.

As opposed to dipole antennas, there are no closed-form analytical equations to govern the design of a patch antenna. There are several approximate models, such as the cavity model [2], but these models are only suited for perfect electric conductor patch antennas and do not account for the multiple complex phenomena that affect patch antennas, namely, the SPR (in the XY-resonance plane) and the Fabry-Perot effect (between ground plane and patch cavity). Due to the complexity in analytically describing these phenomena, finite element methods (FEM) are commonly utilized to design and fine tune the antenna geometry.

In this study, we utilize COMSOL Multiphysics to design a reference gold nano-patch antenna at optical frequencies. After introducing the complex-valued permittivity of gold in the simulation platform, we utilize the S11 parameter, or antenna input port reflection coefficient R_{ant}, as the target performance metric and analyze the impact of the antenna length, width and thickness on the resonant frequency of the antenna and, ultimately, optimize its design. For our target frequency of 200 THz, the antenna design parameters are given in Table 1 and the final S11 parameter is shown in Figure 4.

Parameter	Value
Patch Length	370 nm
Patch Width	300 nm
Stub Length	60 nm
Stub Width	10 nm
Substrate Thickness	50 nm
Antenna Thickness	20 nm
Plasma Frequency	13.35 PHz

Table 1: Design parameters of an optical gold nano-patch antenna resonant at 200 THz.

3 NANO-PATCH ANTENNA AS A BIOSENSOR

Normally, an antenna is designed to resonate at a particular frequency band of interest. The resonant frequency is dependent on the electrical length of the antenna. Thus, if there is a material property which causes a change in the antenna electrical length, the antenna resonant frequency changes too. For optical nano-patch antennas, the thickness and conductivity of the top metallic layer, h_{patch}, affect its electrical length. As a result, a change in the thickness and/or electrical properties of the top metallic layer leads to a change in the antenna effective length. Moreover, as discussed in the previous section, the frequency response of an optical antenna is governed by the propagation properties of SPP waves, and these are dependent and very sensitive to the metal-dielectric interface. Thus, if the dielectric properties of the material surrounding the antenna change, both the plasmonic wavelength and the antenna resonant frequency change too. By leveraging this property, an antenna can be designed to act as a sensor.

SPR-based biosensors have traditionally harnessed the sensitivity of plasmonic waves to the dielectric properties of metal-dielectric interfaces [6, 14, 17]. These sensors rely on the gratings on the metal surface to couple the incident light to plasmonics waves and sensing information is generally carried by reflected signals. These sensors are coated with a biofunctionalized layer that binds only to specific biomarkers. This binding changes the dielectric properties. Through this approach, SPR sensors can offer molecular-level accuracy.

In our antenna numerical model, we capture the impact of molecular binding by changing the antenna thickness, h_{patch}. By changing h_{patch}, we are effectively changing the conductivity of the top metallic layer, mimicking a binding effect. Conducting more accurate simulations would require the selection of specific binding agents, which is part of our ongoing work. The antenna performance as a sensor is evaluated using the FEM and performing a parametric sweep on the antenna thickness in steps of 5 nm. The results are shown in Figure 5. As it can be seen from the figure, as the thickness of the antenna top metallic layer is changed, the resonating frequency of the antenna shifts. A similar effect is also seen when we change the relative permittivity of the dielectric layer

on top of antenna as shown in Figure 6. These effects are leveraged to perform detection.

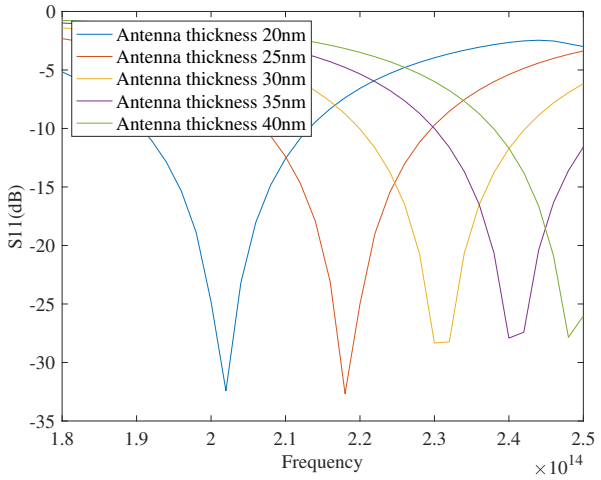

Figure 5: S11 parameter as a function of frequency for different antenna top layer thickness h_{patch}.

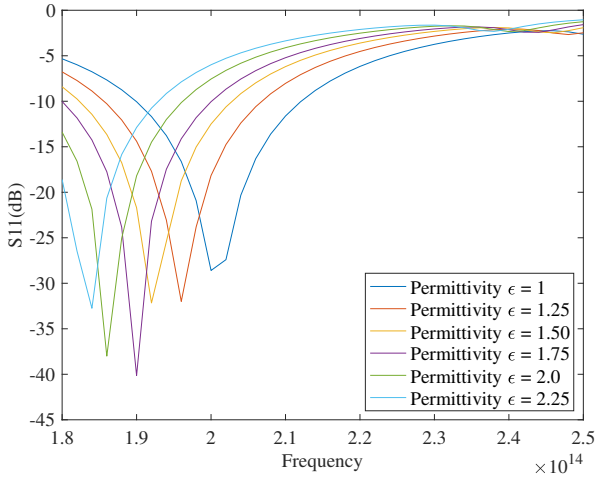

Figure 6: S11 parameter as a function of frequency for different top dielectric layer permittivity.

4 ANTENNA EXCITATION SIGNAL WAVEFORM DESIGN

To successfully detect the change in the antenna resonant frequency and perform sensing, a waveform that can allow for wideband excitation of the antenna is needed. In this section, we propose the utilization of a linear chirp, which is a common waveform leveraged in many sensing applications [3, 7, 10].

In light of the limited capabilities of nanomachines, we are interested in low complexity waveforms. The simplest chirp signals are linear up-chirp and down-chirp waveforms. The frequency of an up-chirp/down-chirp signal increases/decreases with the symbol time. The key parameters of a chirp signal are: the start and stop frequencies, the symbol duration and, correspondingly, the rate or slope of increase or decrease. A chirp signal in time domain is given by:

$$x(t) = \sin\left(\phi_0 + 2\pi f(t)t\right), \tag{7}$$

where ϕ_0 is the initial phase of the signal and

$$f(t) = Ct/2 + f_0, \tag{8}$$

where C is the chirp rate/slope and f_0 is the starting frequency. For linear chirp signals,

$$C = \left(f_1 - f_0\right)/T, \tag{9}$$

where f_1 is the chirp stop frequency and f_0 is the chirp start frequency and T is the time of sweep.

The main advantage of using chirp signal is its ability to sweep a wide frequency. This property is particularly useful for accessing the wideband response from sensing antenna and also makes it immune to any narrow band frequency selectivity introduced by the channel. When transmitting a linear chirp, the sensing nano-antenna frequency response is imprinted on the transmitted waveform. The power spectral density of the transmitted waveform P_t is given by

$$P_t\left(f\right) = P_{chirp}\left(f\right)\left(1 - \left|R_{ant}\left(f\right)\right|^2\right), \tag{10}$$

where P_{chirp} is the power spectral density of generated chirp signal and R_{ant} is the antenna input reflection coefficient or S11 parameter and depends on the sensed information, as described in Section 3.

5 DETECTION MECHANISMS

The sensor-imprinted waveform propagates through the channel and reaches the receiver. We acknowledge that the channel can also alter the waveform in a frequency-selective manner [5], but we leave the study of the impact of the channel for our future work.

To successfully detect the sensors response, we need to extract the antenna resonant frequency from the received signal. This can be done using multiple approaches. On the one hand, a broadband receiver can be utilized to examine the peak power frequency of the received chirp signal via signal processing. Even-though this approach simplifies the receiver physical layer design, it also adds complexity of the required digital signal processing, making its implementation challenging for a nanomachine.

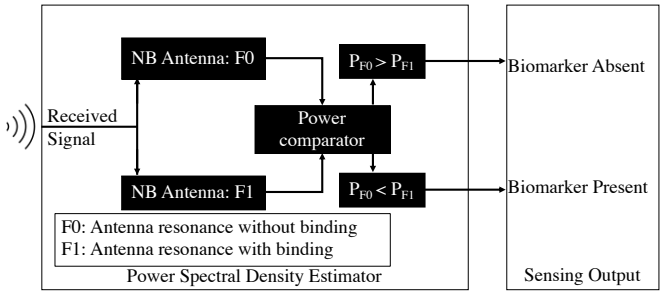

Figure 7: Block diagram of power spectral density estimator of the proposed system for detection in a nano machine.

Another approach to perform broadband detection is with the utilization of an array of narrow-band antennas that act as band pass filters for the received signal. Figure 7 shows a block diagram of such detector based on narrow-band antennas, similar to those proposed in cooperative spectroscopy [4]. Once the signal is received, a simple power detector can be used extract the antenna resonance band. Thus, if a shift in antenna peak resonance band is detected, we can confirm the presence of bio-markers on the antenna.

The main advantage of using an antenna as a sensor is the ability to use the setup for communication while the sensing response is superposed onto that. This makes it an efficient setup for a nanoscale machine, which has strict constraints for the dimensions. Figure 8 presents the block diagram of such detection mechanism.

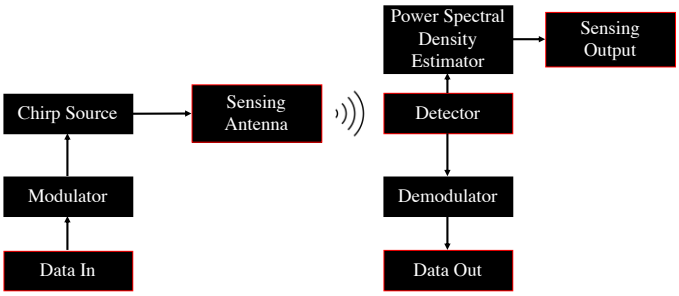

Figure 8: Block diagram of the proposed system for detection and communication.

6 NUMERICAL ANALYSIS

6.1 Antenna chirp excitation

The chirp signal is modelled as per the equation (7) and the single side frequency power spectrum of the chirp is presented in Figure 9. The analyzed chirp sweeps from 180 THz to 250 THz in 2.5 ns. It can be observed that the power of a linear chirp signal is evenly distributed along the swept frequency.

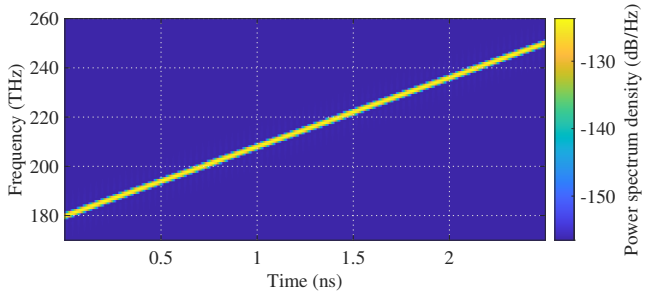

Figure 9: Power spectrum of linear chirp signal used for antenna excitation.

6.2 Imprinted chirp waveform

To analyze the sensing antenna, we need to account for the antenna response and calculate the transmitted power as per equation (10). The power spectrum of the two possible emitted chirp signals, i.e., biomarker bound, and biomarker not bound, is shown in Figure 10. As predicted, the two transmitted waveforms have a very significant power spectral density or electromagnetic signature.

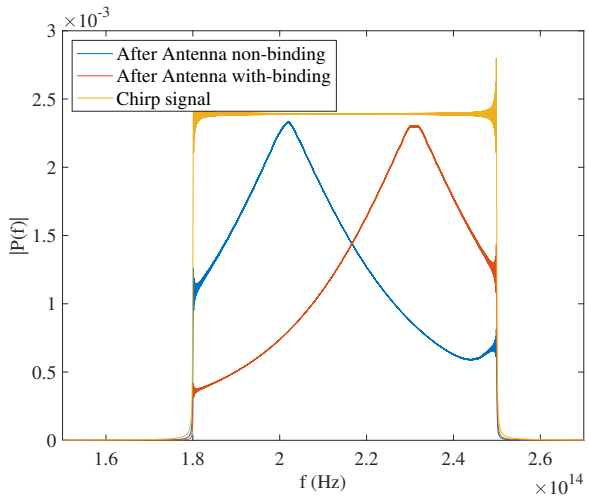

Figure 10: Chirp signal power vs the response of antenna affecting the transmitted signal.

6.3 Chirp detection

To perform successful detection, we rely on computing the power of the resultant signal. The antenna response determines the peak power in the received signal. Any change in the antenna resonant frequency can be detected by detecting the shift in the received signal peak power. To model the peak detection, we used the cutoff power to be -127dB. Thus, only the peak of the signal is detected.

We compare with the case of antenna performance at antenna thickness 20 nm and 30 nm for binding and non-binding analysis. We show the effect of binding on the transmitted signal at receiver in Figure 11a and Figure 11b. This result successfully demonstrates the detection of the shift in antenna resonance from 200THz to 230THz as a result of binding and establish the use of antenna as a sensing element.

6.4 Joint communication and sensing

For communication using chirp we can utilize up-chirp and down-chirp signals to encode the data. An up-chirp can represent a binary '1' while a down-chirp symbol can represent '0'. Thus, data can be transmitted from the transmitter to receiver and by analyzing the peak power of the received signal we can perform detection for the bio-marker. In Figure 12a and Figure 12b, a data packet modulated as per the chirp modulation scheme transmitted through the antenna acting as a sensor is shown. The effects of the binding verses non-binding cases can be observed in the transmitted signals. The bandwidth of the initial chirp and that of each individual antenna can be jointly designed to minimize the effective transmission power loss due to antenna filtering issues. This is part of the future work.

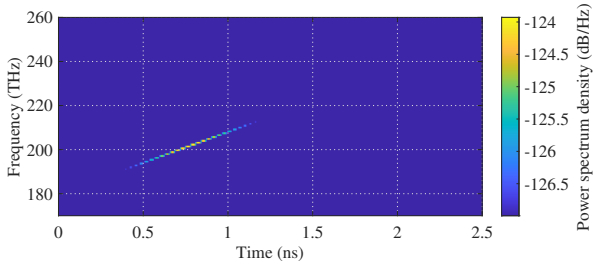

(a) No biomarker binding.

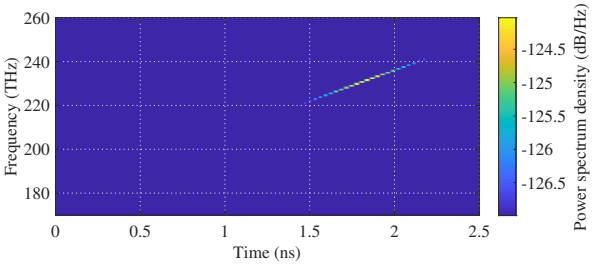

(b) With biomarker binding.

Figure 11: Detection of antenna resonant frequency before and after binding based on the cutoff frequency and power spectrum.

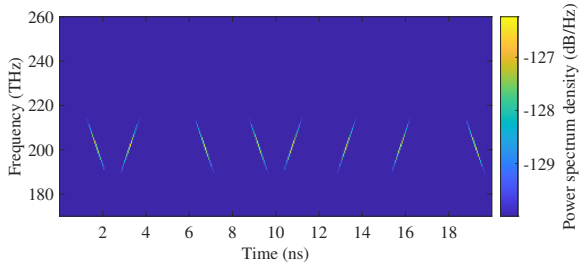

(a) No biomarker binding.

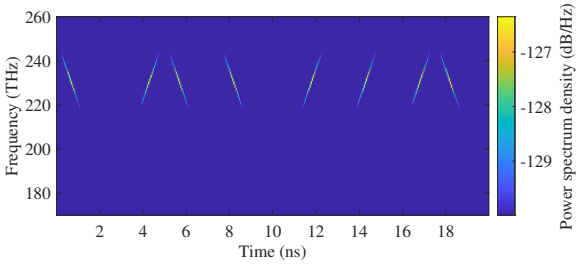

(b) With biomarker binding.

Figure 12: Data packet (01001110) transmitted using chirp modulation scheme.

7 CONCLUSIONS

In this paper, we have proposed and numerically investigated the concept of joint nanoscale communication and sensing enabled by plasmonic nano-antennas. For this, we have studied the impact that changing the conductivity of the top layer of an optical nano-patch antenna has on its frequency and showed how that information is embedded on the power spectral density of the transmitted waveforms. We have then proposed the utilization of broadband chirp signals and suggested a practical nanomachine-ready mechanisms to estimate the power spectral density. There are many research opportunities arising from this work, including the optimization of the chirp waveform and the bandwidth of the patch antennas to jointly maximize the sensing accuracy and minimize the communication bit error rate.

ACKNOWLEDGEMENT

This work was supported by U.S. National Science Foundation (NSF) under grant no. IIP-1718177, CBET-1706050 and CBET-2039189.

REFERENCES

[1] Ian F Akyildiz and Josep Miquel Jornet. 2010. Electromagnetic wireless nanosensor networks. *Nano Communication Networks* 1, 1 (2010), 3–19.
[2] A Balanis Constantine et al. 2005. Antenna theory: analysis and design. *MICROSTRIP ANTENNAS, third edition, John wiley & sons* (2005).
[3] Eyal Gerecht, Kevin O Douglass, and David F Plusquellic. 2011. Chirped-pulse terahertz spectroscopy for broadband trace gas sensing. *Optics express* 19, 9 (2011), 8973–8984.
[4] Hongzhi Guo, Josep Miquel Jornet, Qiaoqiang Gan, and Zhi Sun. 2017. Cooperative Raman spectroscopy for real-time in vivo nano-biosensing. *IEEE transactions on nanobioscience* 16, 7 (2017), 571–584.
[5] Pedram Johari and Josep Miquel Jornet. 2017. Nanoscale optical wireless channel model for intra-body communications: Geometrical, time, and frequency domain analyses. *IEEE Transactions on Communications* 66, 4 (2017), 1579–1593.
[6] J. R. Mejía-Salazar and Osvaldo N. Oliveira. 2018. Plasmonic Biosensing. *Chemical Reviews* 118, 20 (Oct 2018), 10617–10625. https://doi.org/10.1021/acs.chemrev.8b00359
[7] Mart Min, R Land, T Paavle, T Parve, P Annus, and D Trebbels. 2011. Broadband spectroscopy of dynamic impedances with short chirp pulses. *Physiological measurement* 32, 7 (2011), 945.
[8] Eden Morales-Narváez and Can Dincer. 2020. The impact of biosensing in a pandemic outbreak: COVID-19. *Biosensors and Bioelectronics* 163 (2020), 112274.
[9] Mona Nafari and Josep Miquel Jornet. 2017. Modeling and performance analysis of metallic plasmonic nano-antennas for wireless optical communication in nanonetworks. *IEEE Access* 5 (2017), 6389–6398.
[10] G Barratt Park and Robert W Field. 2016. Perspective: The first ten years of broadband chirped pulse Fourier transform microwave spectroscopy. *The Journal of chemical physics* 144, 20 (2016), 200901.
[11] Priyangshu Sen, Honey Pandey, and Josep M Jornet. 2020. Ultra-broadband chirp spread spectrum communication in the terahertz band. In *Next-Generation Spectroscopic Technologies XIII*, Vol. 11390. International Society for Optics and Photonics, 113900G.
[12] Ashkan Shafiee, Elham Ghadiri, Jareer Kassis, Nima Pourhabibi Zarandi, and Anthony Atala. 2018. Biosensing Technologies for Medical Applications, Manufacturing, and Regenerative Medicine. *Current Stem Cell Reports* 4, 2 (Jun 2018), 105–115. https://doi.org/10.1007/s40778-018-0123-y Company: Springer Distributor: Springer Institution: Springer Label: Springer number: 2 publisher: Springer International Publishing.
[13] GI Stegeman, JJ Burke, and DG Hall. 1982. Nonlinear optics of long range surface plasmons. *Applied Physics Letters* 41, 10 (1982), 906–908.
[14] Mark I. Stockman. 2015. Nanoplasmonic Sensing and Detection. *Science* 348, 6232 (April 2015), 287–288. https://doi.org/10.1126/science.aaa6805
[15] Frank Vollmer and Lan Yang. 2012. Review Label-free detection with high-Q microcavities: a review of biosensing mechanisms for integrated devices. *Nanophotonics* 1, 3–4 (Dec 2012), 267–291. https://doi.org/10.1515/nanoph-2012-0021
[16] Eisa Zarepour, Mahbub Hassan, Chun Tung Chou, and Adesoji A Adesina. 2017. Semon: Sensorless event monitoring in self-powered wireless nanosensor networks. *ACM Transactions on Sensor Networks (TOSN)* 13, 2 (2017), 1–28.
[17] Xie Zeng, Yunchen Yang, Nan Zhang, Dengxin Ji, Xiaodong Gu, Josep Miquel Jornet, Yun Wu, and Qiaoqiang Gan. 2018. Plasmonic interferometer array biochip as a new mobile medical device for cancer detection. *IEEE Journal of Selected Topics in Quantum Electronics* 25, 1 (2018), 1–7.